



Scientia Agropecuaria

Web page: <http://revistas.unitru.edu.pe/index.php/scientiaagrop>

Facultad de Ciencias
Agropecuarias

Universidad Nacional de
Trujillo

RESEARCH ARTICLE



Intelligent biofilm with blueberry extract, rice straw nanocellulose and polyvinyl alcohol: Characterization and its application in visual freshness monitoring in tilapia fillets

B. A. Viloché-Villar¹ ; M. P. Obando-Padilla¹ ; D. A. Medina-Bocanegra¹ ; Hernán Alvarado-Quintana¹ ; F. J. Hurtado-Butrón² ; C. Sopán-Benaute³ ; J. C. Rodríguez-Soto¹ ; Yulissa Ventura-Avalos¹ ; J. C. Alcántara^{1,4} ; F. Vilaseca⁴ ; G. Barraza-Jáuregui^{1*}

¹ Research Group on Biopolymers, Nanomaterials and Technology (GIBINTEC), Facultad de Ciencias Agropecuarias, Universidad Nacional de Trujillo, La Libertad, Peru.

² Nanoscience and Nanotechnology Research Group (GMIN-UNT), Facultad de Ciencias Físicas y Matemáticas, Universidad Nacional de Trujillo, La Libertad, Peru.

³ Research Group on Natural Products and Bioactive Substances (GIPRONAS), Facultad de Farmacia y Bioquímica, Universidad Nacional de Trujillo, La Libertad, Peru.

⁴ Advanced Biomaterials and Nanotechnology (BIMATEC), Department of Chemical and Agricultural Engineering and Agrifood Technology, Universitat de Girona, C/Maria Aurèlia Capmany, 61, 17003 Girona, Spain.

* Corresponding author: gbarraza@unitru.edu.pe (G. Barraza-Jáuregui).

Received: 21 January 2025. Accepted: 7 March 2025. Published: 24 March 2025.

Abstract

Intelligent packaging represents a sustainable solution for food preservation by enabling the monitoring of freshness through chromatic changes. In this study, a biofilm based on polyvinyl alcohol (PVA), nanocellulose (NC) extracted from rice straw and blueberry extract was developed and evaluated for its performance as a visual freshness indicator in tilapia fillets. Nanocellulose, obtained by TEMPO oxidation, exhibited proper integration into the polymeric matrix according to transmission electron microscopy, Fourier transform infrared spectroscopy, thermogravimetric analysis and X-ray diffraction analysis. The biofilms improved their mechanical properties with the addition of NC, by increasing tensile strength and reducing water solubility. However, the incorporation of anthocyanins increased solubility and water vapor permeability due to their hydrophilic character. Despite this, their high chromatic sensitivity to pH allowed for color changes: red in acidic media (pH 2-4) and green/brown in alkaline media (pH > 9). These visual changes validate the potential of anthocyanins as freshness indicators, positioning biofilms as a functional and sustainable alternative to conventional packaging. In addition to enabling real-time monitoring, these biofilms can contribute to reducing food waste and fostering more sustainable solutions in the packaging industry, with significant potential for innovative commercial applications.

Keywords: *Vaccinium corymbosum*; nanotechnology; thermal degradation; mechanical properties; pH indicator; sustainability.

DOI: <https://doi.org/10.17268/sci.agropecu.2025.016>

Cite this article:

Viloché-Villar, B. A., Obando-Padilla, M. P., Medina-Bocanegra, D. A., Alvarado-Quintana, H., Hurtado-Butrón, F. J., Sopán-Benaute, C., Rodríguez-Soto, J. C., Ventura-Avalos, Y., Alcántara, J. C., Vilaseca, F., & Barraza-Jáuregui, G. (2025). Intelligent biofilm with blueberry extract, rice straw nanocellulose and polyvinyl alcohol: Characterization and its application in visual freshness monitoring in tilapia fillets. *Scientia Agropecuaria*, 16(2), 189-202.

1. Introduction

In recent decades, food packaging has undergone significant evolution, extending beyond its traditional role of product preservation, integrating intelligent solutions aimed at monitoring quality, safety, and integrity throughout the supply chain (Lim et al., 2024). This advancement addresses global challenges, including the reduction of food

waste, the enhancement of sustainability, and the prevention of foodborne illnesses (Liu et al., 2021). Among these innovations, intelligent packaging stands out for providing visual information of food condition through physical or chemical changes, while also representing a biodegradable and functional alternative to conventional materials (Yan et al., 2021).

Typically, these packaging materials consist of a biodegradable solid matrix combined with colorants sensitive to pH variations (Liu et al., 2021). Among the solid matrices employed, polyvinyl alcohol (PVA), a polymer renowned for its flexibility, mechanical strength, and film-forming capacity, though it faces limitations in humid environments (Koshy et al., 2024). To mitigate these drawbacks, the incorporation of nanocellulose (NC), a promising eco-friendly nanomaterial, as a structural reinforcement has been demonstrated to significantly enhance the mechanical and barrier properties of the films (Mahardika et al., 2024). On the other hand, natural extracts rich in anthocyanins offer an innovative approach for monitoring food freshness, as these compounds exhibit color changes in response to pH variations. These chromatic transitions enable differentiation between fresh and spoiled food (Cheng et al., 2022; Koshy et al., 2024). Despite advancements in the development of intelligent biofilms containing anthocyanins, few studies have analyzed the performance of films composed of PVA, rice straw nanocellulose, and blueberry extract under realistic storage conditions. Therefore, the present study aims to develop and characterize an intelligent biofilm composed of PVA, rice straw nanocellulose, and blueberry extract, evaluating its physical and mechanical properties, as well as its capacity to visually monitor the freshness of tilapia fillets. This approach seeks to offer an innovative and sustainable solution for the food industry, promoting the use of biodegradable materials and contributing to food waste reduction.

2. Methodology

Biological material

Rice straw fibers were used with the following structural composition: moisture: $8.12 \pm 0.22\%$; ash: $26.19 \pm 0.20\%$; extractives: $11.47 \pm 0.23\%$; proteins: $3.19 \pm 0.03\%$; acid-insoluble lignin: $7.40 \pm 0.11\%$; acid-soluble lignin: $2.58 \pm 0.01\%$; structural carbohydrates: $45.36 \pm 0.27\%$; other components: $3.82 \pm 0.23\%$ (Haro et al., 2024). Additionally, discarded blueberry of Biloxi variety was sourced from agro-industrial companies in La Libertad Region, Peru (Haro et al., 2024; Zevallos et al., 2020).

Extraction and characterization of nanocellulose from rice straw

Rice straw (RS) was processed by grinding (IKA Multidrive Basic M20, Germany) and sieved through a No. 30 sieve (600 μm). Subsequently, the fibers were subjected to extraction with 96% ethanol (10:90, v/v) in an autoclave at 121°C for 2 hours to

remove lignin, pectin, waxes, and fats. After extraction, the material was filtered and washed until the supernatant became clear, while the resulting sediment was dried in an oven (Memmert UF260 Plus, Germany).

For bleaching, a solution of sodium chlorite (1%) and acetic acid (1%) at a 1:20 ratio (based on solids) was used, under constant stirring (IKA CMAG HS7 Control magnetic stirrer, Germany) at 60°C for 2 hours. Subsequently, the fibers were washed with distilled water until the pH reached 5.5, filtered, and stored in sterile glass containers at 4°C .

Cellulose nanofibers (NC) were obtained through (2,2,6,6-tetramethylpiperidin-1-yl)oxyl (TEMPO)-mediated oxidation, following the protocol of Alcántara et al. (2020). For this, 1 g of bleached fibers (dry weight) was suspended in 200 mL of water containing TEMPO (0.016 g, 0.01 mmol) and sodium bromide (0.1 g, 1 mmol). Sodium hypochlorite (10 mM) was added under constant stirring (500 rpm), maintaining the pH between 10 and 11 by gradually adding 0.5 N NaOH. At the end of the process, the pH was adjusted to 7 using 1 M HCl.

The oxidized fibers were washed with distilled water and centrifuged (10,000 rpm, 20 minutes) to remove residual reagents. Subsequently, a 1% (w/w) suspension was prepared and homogenized using an Ultraturrax (IKA T25, Germany) at 15,000 rpm for 15 minutes to obtain a homogeneous cellulose nanofiber gel, which was stored at 4°C for further use.

The characterization of the nanofibers was carried out using transmission electron microscopy (TEM, Hitachi S-4800, Japan), Fourier transform infrared spectroscopy (FTIR), and X-ray diffraction. These techniques allowed for the evaluation of the morphology, chemical composition, and crystalline structure of the nanofibers.

Preparation of blueberry anthocyanin extract

The anthocyanin extract (AE) was obtained following the method of Cheng et al. (2022). Blueberry fruits (Biloxi variety) were frozen at -40°C and lyophilized (Labconco, 7806030, USA). The dried material was then ground and stored at 4°C in airtight dark glass containers to prevent light-induced degradation.

For extraction, a mixture of crushed blueberry and 80% ethanol (pH 2) was prepared at a 1:9 (w/w) ratio. The mixture was stirred for 3 hours and then filtered to obtain the AE, which was stored at 4°C , following the procedure adapted from Zevallos et al. (2020).

Anthocyanin quantification was performed using the differential pH method and expressed as cyanidin-3-glucoside (Giusti & Wrolstad, 2001).

Preparation of biofilms

Biofilms were prepared according to the methodology proposed by He et al. (2022), with slight modifications (Figure 1). 4% (w/w) polyvinyl alcohol (PVA) solution was prepared by heating at 80 °C under constant stirring for 30 minutes. Then, different concentrations of nanocellulose (NC) gel: 0.2%, 0.4%, and 0.6% (w/w; db, relative to the PVA weight) were incorporated, designated as PVA/NC I, PVA/NC II, and PVA/NC III, respectively, to evaluate their influence on the mechanical, physical, and functional properties of the material. The mixture was then homogenized for 60 minutes to ensure uniform dispersion.

Additionally, the temperature was reduced to 40 °C, and glycerol was added as a plasticizer at a concentration of 25.2% (w/w relative to PVA). The mixture was stirred for an additional 30 minutes to ensure proper integration of the plasticizer.

For PVA/NC/A III biofilms, blueberry extract (40 mg anthocyanins/mL, equivalent to 20% w/w relative to total weight) was added before incorporating glycerol. This extract, which provides visual detection properties for pH variations, was stirred for 15 minutes to ensure homogeneous dispersion. Glycerol was then added, followed by an additional 30 minutes of stirring.

Film-forming solutions (13 g) were poured into 9 cm diameter Petri dishes and dried in an oven at 35 °C for 48 hours. The dried films were carefully peeled off and stored in metallized airtight bags to protect them from light. Before characterization, the films were conditioned in airtight desiccators at 25 ± 2 °C and 57% relative humidity for 24 hours. Pure PVA films were used as controls, following the methodologies of Sarwar et al. (2018) and Yan et al. (2021).

Transmission electron microscopy

The RS NC sample was observed using transmission electron microscopy (TEM) (EM 910, Zeiss, Jena, Germany). Sample preparation involved diluting NC gel suspensions 10-fold in distilled water. Subsequently, 8 μ L of the diluted nanocellulose suspension was deposited onto the grid membrane and, after drying, stained with a 1% uranyl acetate solution for 3 minutes. Excess stain was removed with absorbent paper before observation (Alcántara et al., 2020).

Scanning electron microscopy (SEM)

The surface morphology of PVA/NC and PVA/NC/A films was examined using a scanning electron microscope (Tescan, Vega 3 LMU, Czech Republic). The sample was coated with a thin conductive gold layer (Qiao et al., 2024).

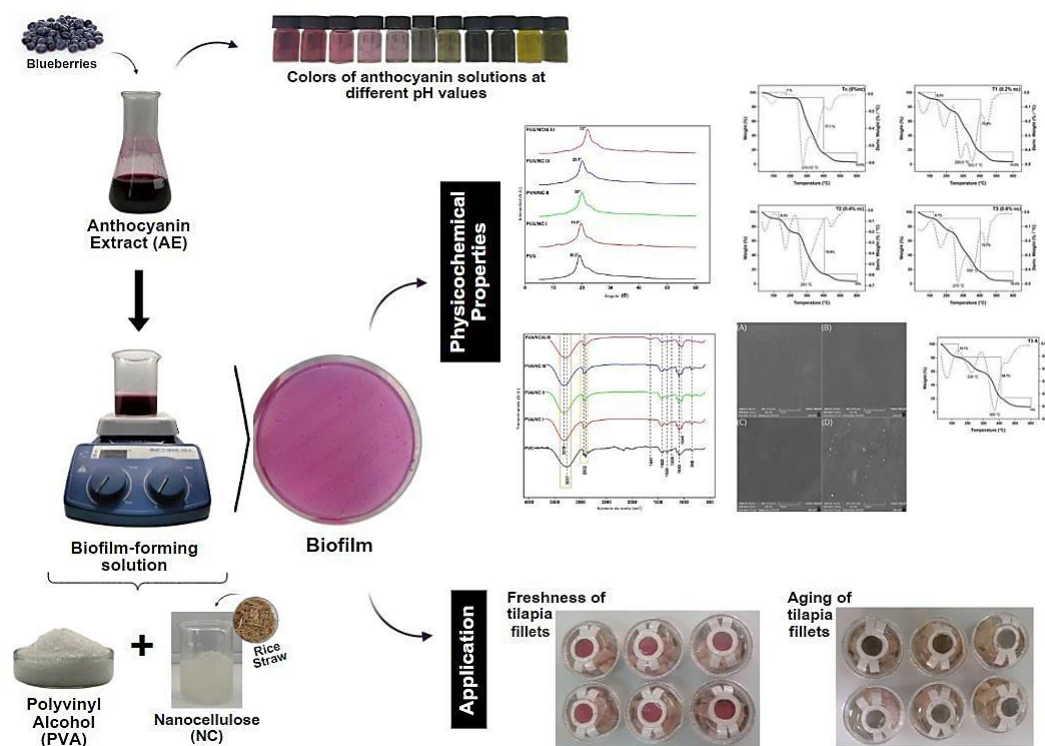


Figure 1. Preparation Process of PVA/NC/A biofilms.

Fourier transform infrared spectroscopy (FTIR)

FTIR spectra of the RS NC sample and PVA/NC and PVA/NC/A films were obtained in the 4000 – 600 cm^{-1} range with a resolution of 4 cm^{-1} using a Fourier transform infrared spectrophotometer (Thermo Scientific, Nicolet iS50, USA) in attenuated total reflectance (ATR) mode (Chen et al., 2020).

X-ray diffraction

X-ray diffraction patterns of the NC sample, PVA/NC, and PVA/NC/A films were obtained using an X-ray diffractometer (Rigaku, Miniflex 600, USA) equipped with copper radiation, applying a voltage of 40.0 kV, a current of 20 mA, and a wavelength of $\lambda = 1.5406 \text{ nm}$. The analysis was performed with scans in a range of 2θ of $5^\circ - 50^\circ$, with a scanning speed of $2^\circ/\text{min}$ (Chen et al., 2020).

Thermogravimetric analysis (TGA)

Thermogravimetric analysis of RS NC and PVA/NC and PVA/NC/A biofilms was performed using a TGA Q5000 analyzer (TA Instruments, USA). Samples (4–5 mg) were placed in aluminum trays and heated under nitrogen flow (40 mL/min) from 30 to 650°C at a heating rate of $5^\circ\text{C}/\text{min}$. The weight loss rate (WLR) analysis was performed from the first derivative of the mass loss curve (He et al., 2022).

Mechanical properties

Tensile strength, elongation at break (%), and Young's modulus of PVA, PVA/NC, and PVA/NC/A biofilms were measured using a texture analyzer (TA-HD Plus, Stable Micro Systems, UK). Samples were cut into $5.0 \times 2.0 \text{ cm}$ pieces, and measurements were performed at a deformation speed of 8.3 mm/s with a 100 kgf load cell (ASTM, 1995; Sarwar et al., 2018).

Water vapor permeability of the biofilms

The permeability of the biofilms was determined gravimetrically at 25°C , adapting the procedure recommended by the ASTM E96-00 standard (ASTM, 2000).

Water solubility of biofilms

The method described by Li et al. (2023) was adapted to determinate the water solubility of films. Films were cut into $15 \times 40 \text{ mm}$ samples and dried in a forced-air oven at 50°C (Memmert, UF260 Plus, Germany) until equilibrium was reached (idm). The dried films were then immersed in 50 mL of distilled water in hermetically sealed beakers to prevent water evaporation and stored at room temperature for 24 hours with gentle periodic agitation. After immersion, the samples were drained, dried at 50°C until reaching a constant weight, and then reweighed (edm) (Equation 1).

$$\text{Solubility (\%)} = \frac{\text{idm} - \text{edm}}{\text{idm}} \times 100 \dots (1)$$

Color and UV-Vis spectrum of anthocyanin solutions at different pH

The pH sensitivity of the anthocyanin extract was evaluated following the protocol described by Oktay et al. (2023), with modifications. Anthocyanin extract (40 mg/mL) (10 mL) was mixed with 30 mL of phosphate buffer (pH 2 – 12) for 10 minutes, followed by the examination of spectra using a UV-Vis spectrophotometer (Thermo Scientific, Genesis 150, USA) after the color reactions.

Application of biofilms for monitoring the freshness of tilapia fillets

Tilapia fillets (100 g) were stored in 250 g plastic containers with a biofilm adhered to the inside the lid, without direct contact with the sample, at 25°C for 24 hours. Sensory quality of the fillet was evaluated every 2 hours following the NTP: 041.001:2019 standard, considering color and odor. Additionally, the color parameters L^* (lightness), a^* (red-green), and b^* (yellow-blue) were measured using a colorimeter (CM-5, Konica Minolta, Japan), with a white standard plate as a reference. The total color difference (ΔE) was calculated using equation 2.

$$\Delta E = [(L - L_0)^2 + (a - a_0)^2 + (b - b_0)^2]^{1/2} \dots (2)$$

L , a , and b represent the color parameters of the biofilms at each evaluation time, while L_0 , a_0 , and b_0 correspond to the initial color values (Chen et al., 2020). During sampling, each process was repeated six times.

Statistical analysis

Results were expressed as the mean-standard deviation. Significant differences among data were determined using Duncan's multiple range tests and were defined at $p < 0.05$.

3. Results and discussion

Characterization of rice straw nanocellulose

Figure 2A presents TEM micrographs of the NC extracted from RS. Morphological analysis revealed that the nanofibers exhibited an average diameter of $80 \pm 12 \text{ nm}$ and an average length of $10.5 \pm 1.6 \text{ nm}$. These values fall within the expected range for cellulose nanofibers (1 – 100 nm), which is consistent with the findings reported of Khalil et al. (2023).

FTIR spectroscopy analysis (Figure 2B) confirmed the presence of characteristic functional groups of cellulose and nanocellulose. The following main peaks were identified: an intense peak in the $3200 - 3600 \text{ cm}^{-1}$ region, attributed to hydroxyl (O-H) groups associated with cellulose; a peak in the $2800 - 3000 \text{ cm}^{-1}$ range, corresponding to C-H

stretching vibrations typical of organic compounds. A peak in the $1000 - 1200 \text{ cm}^{-1}$ region, associated with C-O stretching vibrations in the cellulosic structure. These spectra align with previous studies on nanocellulose extracted from various sources (Jiang & Gu, 2020; Nasution et al., 2022).

X-ray diffraction (XRD) analysis of RS NC (Figure 2C) revealed two prominent crystalline peaks at 15.6° and 21.9° , corresponding to the (110) and (200) crystalline planes of type I cellulose, respectively. These results are characteristic of the native cellulose crystalline structure and are consistent with the findings reported by Khalil et al. (2023) and Nagarajan et al. (2019).

Biofilm analysis

Scanning Electron Microscope (SEM)

Figure 3 obtained by SEM analysis of the surface morphology of PVA (A), PVA/NC I (B), PVA/NC II (C), and PVA/NC III (D) films, revealed specific microstructural characteristics. The PVA (A) film exhibited a uniform and homogeneous surface, as did the films with 0.2% (B) and 0.4% (C) NC addition. However, at a higher NC concentration of 0.6% (D), slight surface irregularities were observed, revealing the identification of some nanofibers and

contributing to a rougher texture. These results align with the findings of Qiao et al. (2024), who demonstrated, through SEM images, that increasing NC content in PVA films leads to increased surface roughness.

FTIR analysis of the biofilms

Figure 4 presents the FTIR spectra of PVA, PVA/NC, and PVA/NC/A biofilms. In the spectrum of the PVA biofilm, characteristic peaks were identified. A maximum absorption peak at 1080 cm^{-1} was attributed to C-O bond stretching, while the peak at 1425 cm^{-1} corresponded to CH-CH₂ bending vibrations, confirming the carbon skeleton structure of PVA. Additionally, a peak at 3257 cm^{-1} , associated with the stretching vibration of -OH groups, was observed (Mahardika et al., 2024).

With the incorporation of NC into the biofilms (PVA/NC I, PVA/NC II, and PVA/NC III), the peak at 3257 cm^{-1} shifted to 3319 cm^{-1} and became more defined, which is attributed to the high hydroxyl group content in NC. This interaction promoted the formation of hydrogen bonds with PVA, as also reported in previous studies (Dong et al., 2022). This shift suggests improved compatibility between the PVA matrix and NC, potentially enhancing the mechanical and barrier properties of the biofilms.

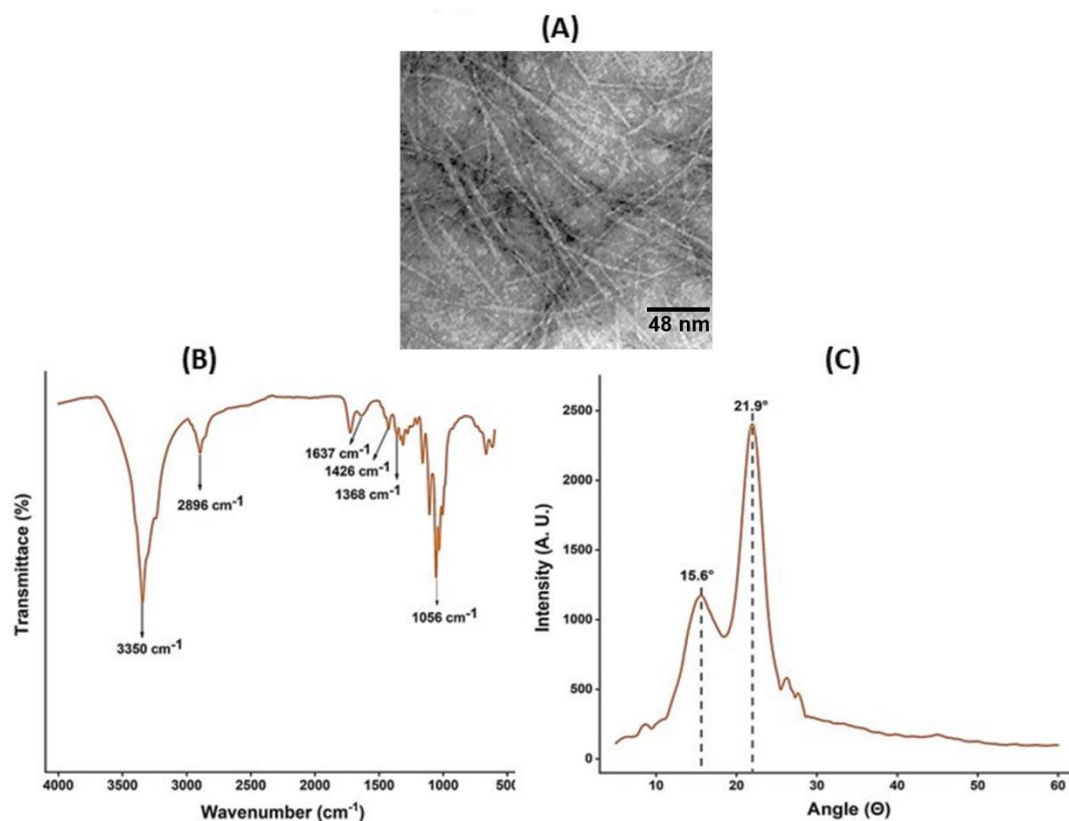


Figure 2. TEM micrographs (A), FTIR spectrum (B), and X-ray diffraction pattern (C) of rice straw nanocellulose.

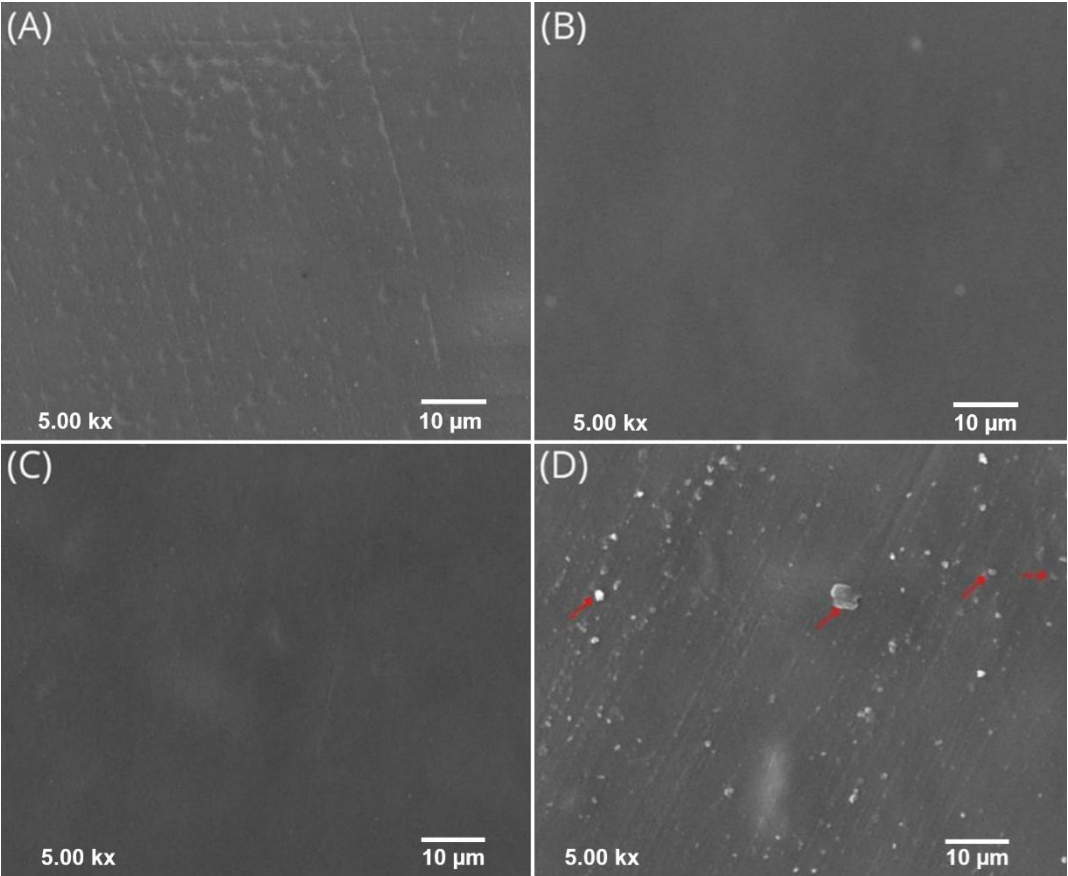


Figure 3. SEM images of the biofilm surfaces: PVA (A), PVA/NC I (B), PVA/NC II (C), and PVA/NC III (D).
*PVA/NC I: NC: 0.2% NC; PVA/NC II: 0.4% NV; PVA/NC III: 0.6% NC.

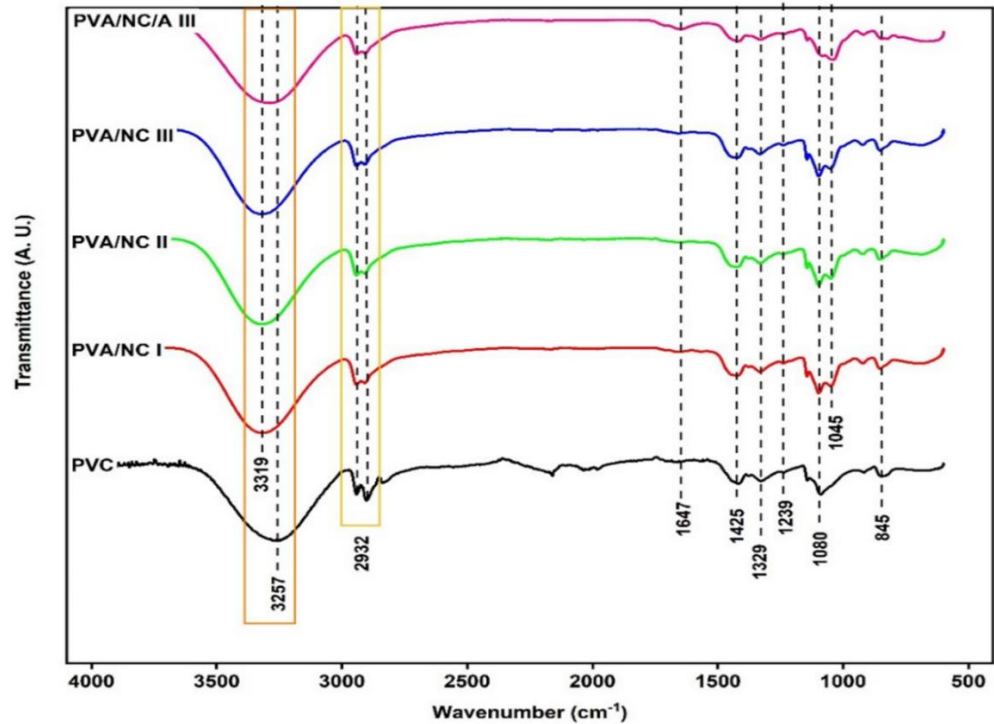


Figure 4. FTIR spectra of PVA, PVA/NC I, PVA/NC II, PVA/NC III, and PVA/NC/A III biofilms.
*PVA/NC I: 0.2% NC; PVA/NC II: 0.4% NC; PVA/NC III: 0.6% NC.

In the spectrum of the PVA/NC/A III biofilm, a new peak emerged at 1627 cm^{-1} , indicative of interactions between the -OH groups of the PVA/NC matrix and the aromatic compounds of the anthocyanin extract. This shift suggests the formation of covalent crosslinks, likely resulting from the protonation of hydroxyl groups in anthocyanins (Zheng et al., 2024). Such covalent bonds could improve the chemical and thermal stability of the biofilms (Zhai et al., 2017).

X-ray diffraction

Figure 5 presents the X-ray diffraction (XRD) patterns of the evaluated biofilms. In the case of pure PVA films, a sharp diffraction peak at 19.2° was identified, characteristic of the polymer's semi-crystalline structure (Zhai et al., 2017). This peak reflects the ordered arrangement of molecular chains within the PVA matrix.

In the PVA/NC biofilms, a shift of this peak toward higher diffraction angles was observed. This phenomenon can be attributed to the incorporation of NC, whose rigid structure and high hydroxyl group content promote hydrogen bond formation with

PVA chains. These interactions hinder the molecular rearrangement of the polymer, leading to increased structural compaction within the matrix (Dong et al., 2022; Zhu et al., 2022).

Similarly, the XRD patterns of PVA/NC/A biofilms did not exhibit additional peaks, indicating that the incorporation of anthocyanins does not significantly alter the crystalline organization of the biofilms. However, an additional shift of the crystalline peak toward higher angles was detected, which could be associated with interactions between the hydroxyl groups of anthocyanins and the PVA/NC matrix. These interactions, likely mediated by hydrogen bonding, enhance structural compaction, further restricting molecular motion within the matrix (Li et al., 2023).

Overall, the modifications observed in the XRD patterns suggest that the incorporation of NC and anthocyanins influences the crystalline organization of the biofilms, which could directly impact their mechanical and barrier properties. These findings reinforce the potential of these biofilms for advanced applications in intelligent packaging.

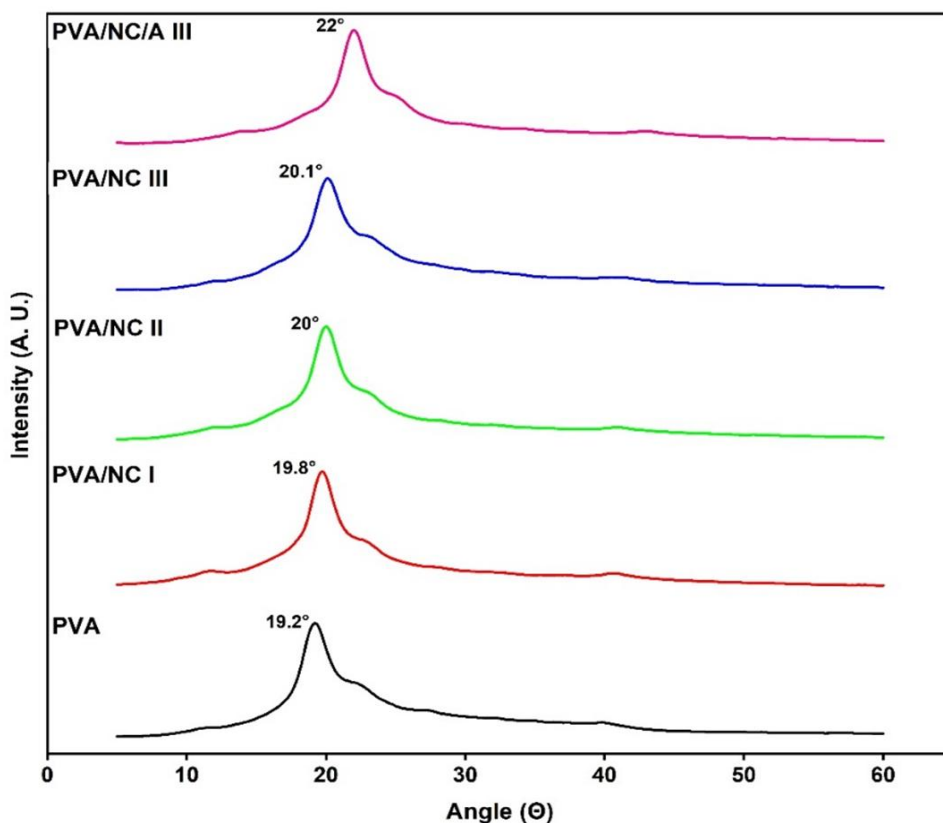


Figure 5. X-ray diffraction pattern of PVA, PVA/NC I, PVA/NC II, PVA/NC III and PVA/NC/A III biofilms
*PVA/NC I: 0.2% NC; PVA/NC II: 0.4% NC; PVA/NC III: 0.6% NC.

Thermogravimetric analysis and DTG

Table 1 presents the thermogravimetric analysis (TGA) and weight loss rate (DTG) of the evaluated biofilms, identifying three distinct degradation stages.

The first stage occurs between approximately 30 °C and 176.2 °C, with a weight loss ranging from 7% to 18.1%, depending on the treatment. This phase is mainly associated with the removal of absorbed water by the biofilms, as well as the release of volatile compounds and short-chain oligomers (He et al., 2022; Li et al., 2022). In particular, the PVA/NC/A III film exhibited significantly weight loss (18.1%), suggesting an increased release of moisture and volatile compounds derived from anthocyanins.

The second degradation stage occurs between 134.8 °C and 406 °C, depending on the biofilm formulation. During this phase, cleavage of the main PVA chain and the breakdown of the nanocellulose structure take place. In biofilms containing nanocellulose (PVA/NC II and PVA/NC III), this phase was delayed until 219.1 °C, indicating a stabilizing effect. However, in the PVA/NC/A III film, degradation initiated at a lower temperature (141.1 °C), suggesting that anthocyanins promote early thermal degradation. This effect is likely due to their conversion into aldehydes and phenolic acids through heat-induced deglycosylation and ring-opening reactions.

The third stage occurs at temperatures above 406 °C, with a weight loss rate ranging between 10% and 14%. At this point, complete carbon bond cleavage and gasification of organic residues take place (Li et al., 2022; Oktay et al., 2023; Zhu et al., 2022). Biofilms containing anthocyanins exhibited the highest weight loss at this stage (14%), indicating that residues formed in the second stage continued to decompose at higher temperatures. The final residue at 600 °C was 2.7%, 4.1%, 4.1%, 7.3%, and 7.4% for PVA, PVA/NC I, PVA/NC II, PVA/NC III, and PVA/NC/A III biofilms, respectively. The increased residual mass in biofilms containing NC suggests enhanced thermal stability due to the presence of carbonaceous structures. In the case of PVA/NC/A III, the final residue is similar to that of

PVA/NC III, indicating that anthocyanin degradation does not significantly contribute to the formation of solid residues. This could be attributed to interactions between anthocyanins and nanocellulose, which facilitate the conversion of pigments into volatile products.

These findings are partially consistent with those reported by He et al. (2022), who demonstrated that the addition of nanocellulose enhances thermal stability in PVA biofilms containing cellulose nanocrystals and anthocyanin extract from red cabbage. In this study, the presence of anthocyanins reduced the degradation temperature in the second stage, suggesting that their influence on thermal stability depends on their chemical structure and interactions with the polymeric matrix.

Mechanical Properties of PVA, PVA/NC, and PVA/NC/A Biofilms

The mechanical properties of the evaluated biofilms are summarized in Table 2. The pure PVA biofilm exhibited the lowest tensile strength (7.137 ± 0.131 MPa) and Young's modulus (10.545 ± 0.101 MPa), indicating a flexible matrix with high elongation ($67.69 \pm 1.747\%$). However, its limited stiffness and strength suggest a weakly reinforced polymeric structure.

The incorporation of NC as a reinforcing agent significantly enhanced the mechanical properties of the biofilms (He et al., 2022). Tensile strength increased progressively with higher NC concentrations, improving by 47%, 75%, and 116% in PVA/NC I, PVA/NC II, and PVA/NC III, respectively, reaching a maximum value of 15.459 ± 0.555 MPa in the PVA/NC III formulation. However, this increase in strength was initially accompanied by an initial reduction in elongation ($37.86 \pm 1.451\%$) in PVA/NC I, which could be attributed to the increased matrix stiffness, as evidenced by the higher Young's modulus (27.691 ± 1.318 MPa).

At higher NC concentrations, elongation recovered significantly, reaching $85.88 \pm 2.941\%$ in PVA/NC III. This could be explained by better dispersion of nanofibers within the matrix, which promotes an optimal balance between strength and flexibility (Zhu et al., 2022).

Table 1

TDA/DTG analysis of PVA, PVA/NC and PVA/NC/A biofilms

Treatments	1st Stage		2nd Stage		3rd Stage		Residue (%)
	T°	Weight loss (%)	T°	Weight loss (%)	T°	Weight loss (%)	
PVA	30-176.2	7	176.2-406	77.1	406-600	13.2	2.7
PVA/NC I	30-134.8	9.3	134.8-406	73.4	406-600	13.2	4.1
PVA/NC II	30-132.3	9.3	219.1-406	76.9	406-600	10	4.1
PVA/NC III	30-123.4	8.7	219.1-406	73.7	406-600	10.3	7.3
PVA/NC/A III	30-141.1	18.1	141.1-406	59.7	406-600	14	7.4

*PVA/NC I: 0.2 % NC; PVA/NC II: 0.4 % NC; PVA/NC III: 0.6 % NC.

Table 2

Mechanical properties of PVA, PVA/NC and PVA/NC/A biofilms

Treatments	Tensile strength (MPa)	Elongation (%)	Young's modulus (MPa)
PVA	7.137 ± 0.131 ^a	67.69 ± 1.747 ^a	10.545 ± 0.101 ^a
PVA/NC I	10.487 ± 0.734 ^b	37.86 ± 1.451 ^b	27.691 ± 1.318 ^b
PVA/NC II	12.503 ± 0.082 ^c	64.51 ± 2.499 ^a	19.405 ± 0.863 ^c
PVA/NC III	15.459 ± 0.555 ^d	85.88 ± 2.941 ^c	18.003 ± 0.343 ^c
PVA/NC/A III	19.504 ± 1.24 ^e	96.49 ± 1.417 ^d	20.229 ± 1.573 ^c

* Data with different superscript letters in the same column indicate significant difference ($p < 0.05$).

**PVA/NC I: 0.2% NC; PVA/NC II: 0.4% NC; PVA/NC III: 0.6% NC.

The incorporation of anthocyanin extract in the PVA/NC III biofilm (PVA/NC/A formulation) exhibited a synergistic effect, enhancing both strength and flexibility. The tensile strength reached 19.504 ± 1.24 MPa, the highest recorded value, while elongation increased to $96.49 \pm 1.417\%$, the highest observed. This behavior suggests that anthocyanins act as plasticizers, reducing matrix stiffness without compromising its strength (He et al., 2022; Zhai et al., 2017). The Young's modulus (20.229 ± 1.573 MPa) reflected a balance between stiffness and elasticity, positioning this formulation as the most suitable for applications requiring multifunctional, durable, and flexible materials.

Water solubility and permeability of biofilms

The solubility of the biofilms exhibited significant variations depending on their composition (Figure 6A). The pure PVA film showed the highest solubility, which can be attributed to its highly hydrophilic nature and the abundance of free hydroxyl groups in its molecular structure (Panda et al., 2022). In contrast, the PVA/NC biofilms resulted in a progressive decrease in solubility as the NC concentration increased. This behavior is likely due to the formation of a three-dimensional network between NC and PVA chains, as well as a decrease in the number of free hydroxyl groups due to hydrogen bond formation, which limits moisture absorption capacity (Lee et al., 2020).

For anthocyanin incorporation, the biofilm with the lowest solubility, the lowest water vapor permeability, and the highest sensitivity to pH variations were selected, as key criteria for intelligent packaging. According to Che Hamzah et al. (2022), the addition of anthocyanin extract could increase water solubility due to the hydrophilic nature of these molecules, a characteristic inherent to pH-indicator films. This property makes such films more suitable for products with limited exposure to direct moisture.

As an application strategy, the films were designed to be placed on the top section of the packaging, where they can detect volatile compounds generated during storage while minimizing direct contact with high-moisture foods, such as fish fillets. This strategic positioning maximizes the functionality of

the films as freshness sensors, ensuring their effectiveness in monitoring volatile compounds in intelligent packaging (Che Hamzah et al., 2022).

Figure 6B presents the results of the water vapor permeability (WVP) analysis of the evaluated biofilms. The incorporation of NC significantly reduced ($p < 0.05$) the WVP of the films, a phenomenon attributed to the formation of more tortuous pathways within the polymeric matrix due to the homogeneous dispersion of cellulose nanofibers. These pathways hinder the diffusion of water vapor molecules, delaying their transport through the material (Patil et al., 2022). Furthermore, as the NC concentration increased, this effect became more pronounced, as the structural network became denser, enhancing the water vapor barrier properties (He et al., 2022).

In contrast, the incorporation of anthocyanin extract in the PVA/NC/A III formulation resulted in a significant increase ($p < 0.05$) in WVP. This increase is likely due to the hydrophilic nature of anthocyanins, which contain a higher number of free hydroxyl groups capable of interacting with water vapor molecules, facilitating their diffusion through the matrix (He et al., 2022). Additionally, this behavior could be associated with a disruption of the structural continuity of the PVA/NC matrix, which reduces the efficiency of the tortuous pathways formed by nanocellulose. Similar results have been reported by Qiao et al. (2024), who observed that the incorporation of hydrophilic compounds into biofilms can increase WVP due to these interactions.

In this regard, the addition of NC improves the water vapor barrier properties of the films, while anthocyanins, despite enhancing their functional sensitivity of the films, could partially compromise this property. These results highlight the importance of balancing functionality and barrier properties in the design of films for specific applications.

Color and UV-Vis spectrum of anthocyanin solutions at different pH values

Figure 7A shows the color variation in anthocyanin solutions extracted from blueberries as a function of pH. Under acidic conditions (pH 2–4), the solutions exhibit red to pink hues, while at pH 4–7 they

display purple tones. At more alkaline pH values (7 – 9), the colors become bluish, and under highly basic conditions (pH 9 – 12), green-yellow hues predominate.

The UV-Vis spectra presented in Figure 7B reveals a shift in the absorption peak from 510 nm (acidic conditions) to 560 nm (alkaline conditions), accompanied by a decrease in absorption intensity. These changes are attributed to structural transformations of the anthocyanins. In acidic media (pH < 4), the flavylium cation predominates, imparting an intense red color. Between pH 4 and 7, an equilibrium is established among the flavylium cation, the

carbinol (colorless) form, and the chalcone (yellowish). Under alkaline conditions (pH > 7), anthocyanins transform into quinonoid anions, generating blue, green, or brown hues (Lim et al., 2024; Yu et al., 2024).

These color variations, which are directly related to the structural changes in anthocyanins, underscore their potential as visual indicators of freshness in the food industry. The ability to change color with pH facilitates the monitoring of quality and spoilage in perishable foods, offering a practical and sustainable solution for intelligent packaging applications (Oktay et al., 2023).

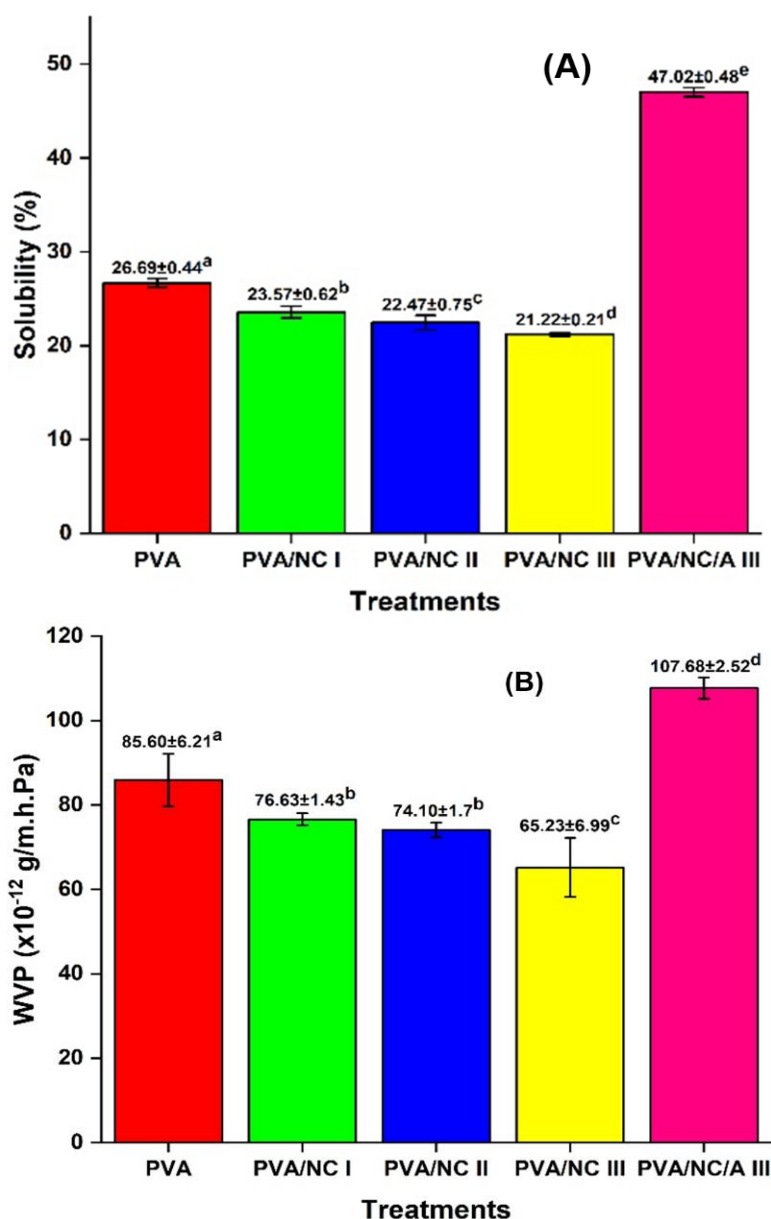


Figure 6. Solubility (A) and water vapor permeability (B) of PVA, PVA/NC and PVA/NC/A biofilms
*PVA/NC I: 0.2 % NC; PVA/NC II: 0.4 % NC; PVA/NC III: 0.6 % NC.

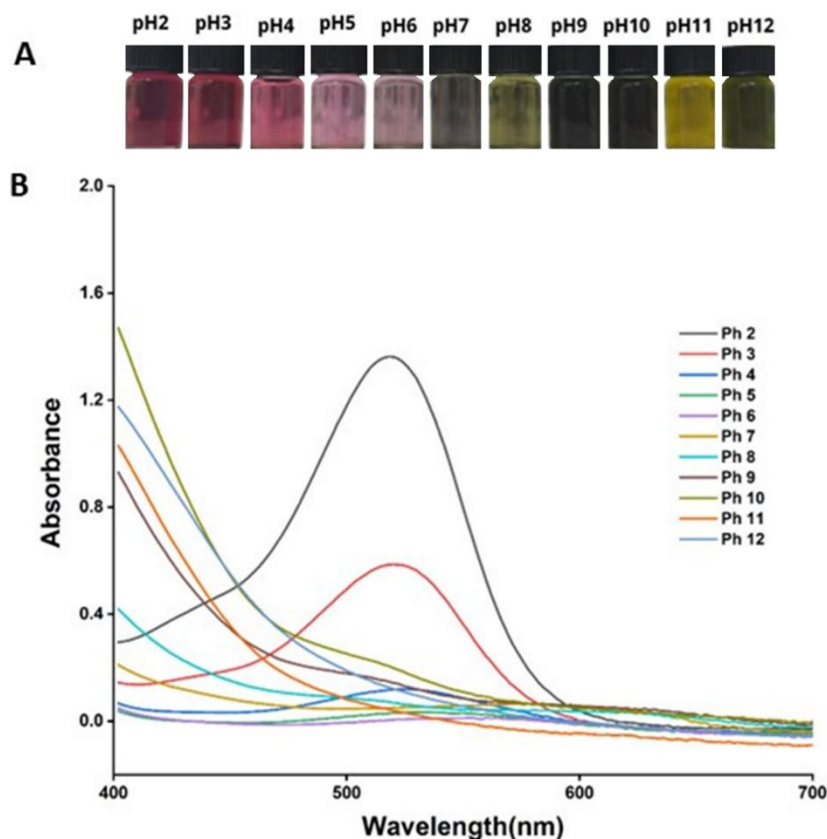


Figure 7. Color (A) and UV-Vis spectrum (B) of anthocyanin solutions at different pH.

Application of biofilms in monitoring the freshness of tilapia filets

Table 3 presents the evolution of the chromatic parameters of the PVA/NC/A III biofilm applied to monitoring the shelf life of tilapia filets. The results indicate that the color changes in the biofilms would be closely related to the release of volatile compounds during the decomposition of tilapia filets, which affect both the pH and the molecular stability of anthocyanins.

The L^* parameter showed an increase from 43.43 (hour 0) to a maximum of 61.49 (hour 16), followed by a slight decrease to 57.22 in hour 18. This increase reflects the progressive degradation of anthocyanin pigments, leading to a lighter coloration over time. The subsequent reduction may be attributed to the accumulation of dark compounds derived from advanced decomposition processes, such as pigmented polymers (Chua et al., 2024).

The a^* parameter initially displayed high positive values (62.84, intense red), progressively decreasing until reaching negative values (-5.56, green) at hour 18. This shift is likely associated with the alkalization of the medium due to the presence of ammonia and volatile amines generated during protein decomposition. Anthocyanins, responsible for red coloration, are highly pH sensitive. Under alkaline

conditions ($pH > 7$), they undergo a transition to quinonoid anion forms, producing greenish tones (Oktay et al., 2023).











The b^* parameter remained negative (bluish) at the beginning (-12.60) but fluctuated and gradually increased to values near zero (0.59) by the end of the evaluation period. The initial coloration corresponds to the characteristics of anthocyanins in acidic or neutral environments (initial pH of fresh fish). As decomposition progresses, the formation of aldehydes and ketones leads to chemical interactions with anthocyanins, promoting a transition toward yellowish tones (Oktay et al., 2023).

The ΔE variation demonstrated a continuous increase from 0 (hour 0) to 71.11 (hour 18), with more pronounced changes after 14 hours. ΔE reflects the overall color change in the biofilms and serves as a visual indicator of fish freshness. The significant increase observed in the final hours could be attributed to the intensified production of volatile compounds (trimethylamine, dimethylamine, and ammonia) which alter the pH and, consequently, the optical properties of anthocyanins (He et al., 2022; Yan et al., 2021).

Similar results in freshness monitoring of shrimp and skinless chicken breasts, have been reported by He et al. (2022) and Oktay et al. (2023), respectively.

Table 3

Chromatic Changes in PVA/NC/A III Biofilms During Monitoring of Tilapia Fillet Freshness

Time	L*	a*	b*	ΔE	Color appearance
0	43.43 ± 0.94	62.84 ± 2.39	-12.60 ± 1.30	-	
2	44.79 ± 4.57	53.75 ± 3.40	-6.34 ± 2.11	11.72 ± 3.91 ^a	
4	49.61 ± 2.77	56.11 ± 4.59	-6.23 ± 1.85	12.58 ± 1.52 ^a	
6	49.85 ± 2.19	56.52 ± 4.35	-6.56 ± 1.88	11.92 ± 2.11 ^a	
8	50.40 ± 3.19	52.13 ± 4.81	-7.10 ± 1.57	15.82 ± 4.41 ^a	
10	51.96 ± 2.89	54.58 ± 2.38	-6.52 ± 1.77	13.85 ± 2.58 ^a	
12	52.78 ± 3.59	47.54 ± 4.81	-8.80 ± 1.88	18.78 ± 5.16 ^a	
14	58.27 ± 4.07	29.61 ± 6.00	-15.45 ± 2.00	36.72 ± 7.22 ^b	
16	61.49 ± 3.80	9.18 ± 9.13	-9.73 ± 5.20	56.99 ± 9.03 ^c	
18	57.22 ± 3.49	-5.56 ± 1.67	0.59 ± 1.34	71.11 ± 2.98 ^d	

4. Conclusions

A intelligent PVA/NC/A III biofilm was developed to monitor the freshness of tilapia fillets through visual chromatic changes. The incorporation of rice straw nanocellulose and blueberry extract enhanced the mechanical and functional properties of the biofilm, achieving a balance between flexibility, strength, and sensitivity. This biofilm exhibited high pH sensitivity, with clear and perceptible color transitions, facilitating its use as a visual freshness indicator for perishable foods.

However, further research is recommended to explore the integration of additional sensors, such as CO₂ and other volatile compound detectors, to develop multiparameter monitoring systems. Moreover, long-term stability tests under various storage conditions should be conducted to validate commercial viability and functionality in different environments.

Acknowledgements

To the National Council for Science, Technology, and Technological Innovation (CONCYTEC), the National Fund for Scientific, Technological, and Technological Innovation Development (FONDECYT), now PROCENCIA, institutions that funded the project "Agro-industrial waste as raw material for the extraction and characterization of nanopolysaccharides" under CONTRACT 402-2019-FONDECYT. Res. Rec. N°105-2020/UNT.

Author contributions

B. A. Viloché-Villar: Methodology, Formal analysis, Research, Visualization; **M. P. Obando-Padilla:** Methodology, Formal analysis, Research, Visualization; **D. A. Medina-Bocanegra:** Methodology, Research, Formal analysis, Writing – Review and Editing; **H. M. Alvarado-Quintana:** Methodology, Formal analysis, Research; **F. J. Hurtado-Butrón:** Methodology, Formal analysis, Research; **C. Sopán-Benaute:** Methodology, Formal analysis, Research. **J. C. Rodríguez-Soto:** Methodology, Formal analysis, Research, Visualization; **Y. Ventura-Avalos:** Methodology, Writing – Review and Editing; **J. C. Alcántara:** Conceptualization, Methodology, Formal analysis, Research; **F. Vilaseca:** Conceptualization, Methodology, Writing – Review and Editing. **G. Barraza-Jáuregui:** Conceptualization, Methodology, Research, Writing – Review and Editing, Resources, Funding Acquisition.

Conflict of interest declaration

The authors declare no conflicts of interest.

ORCID

B. A. Viloché-Villar  <https://orcid.org/0000-0002-2820-1336>
M. P. Obando-Padilla  <https://orcid.org/0000-0003-1813-7489>
D. A. Medina-Bocanegra  <https://orcid.org/0000-0003-0816-1223>
H. M. Alvarado-Quintana  <https://orcid.org/0000-0002-1760-5589>
F. J. Hurtado-Butrón  <https://orcid.org/0000-0002-9449-726X>
C. Sopán-Benaute  <https://orcid.org/0000-0002-0654-5760>
J. C. Rodríguez-Soto  <https://orcid.org/0000-0002-8166-8859>
Y. Ventura-Avalos  <https://orcid.org/0009-0009-7239-433X>
J. C. Alcántara  <https://orcid.org/0000-0002-8261-6452>
F. Vilaseca  <https://orcid.org/0000-0001-7752-3158>
G. Barraza-Jáuregui  <https://orcid.org/0000-0002-0376-2751>

References

- Alcántara, J. C., González, I., Pareta, M. M., & Vilaseca, F. (2020). Biocomposites from Rice Straw Nanofibers: Morphology, Thermal and Mechanical Properties. *Materials*, 13(9), Article 9. <https://doi.org/10.3390/ma13092138>
- ASTM. (1995). *Standard Test Method for Tensile Properties of Thin Plastic Sheeting*.
- ASTM, A. (2000). Standard E96–00. Standard test methods for water vapour transmission of materials. *Annual Book of ASTM Standards*, 4.
- Che Hamzah, N. H., Khairuddin, N., Muhamad, I. I., Hassan, M. A., Ngaini, Z., & Sarbini, S. R. (2022). Characterisation and colour response of smart sago starch-based packaging films incorporated with Brassica oleracea anthocyanin. *Membranes*, 12(10), 913.
- Chen, S., Wu, M., Lu, P., Gao, L., Yan, S., & Wang, S. (2020). Development of pH indicator and antimicrobial cellulose nanofibre packaging film based on purple sweet potato anthocyanin and oregano essential oil. *International Journal of Biological Macromolecules*, 149, 271-280. <https://doi.org/10.1016/j.ijbiomac.2020.01.231>
- Cheng, M., Yan, X., Cui, Y., Han, M., Wang, X., Wang, J., & Zhang, R. (2022). An eco-friendly film of pH-responsive indicators for smart packaging. *Journal of Food Engineering*, 321, 110943. <https://doi.org/10.1016/j.jfoodeng.2022.110943>
- Chua, L. S., Thong, H. Y., & Soo, J. (2024). Effect of pH on the extraction and stability of anthocyanins from jaboticaba berries. *Food Chemistry Advances*, 5, 100835. <https://doi.org/10.1016/j.focha.2024.100835>
- Dong, R., Lu, F., Liu, P., Li, X., Huang, R., Liu, G., & Chen, J. (2022). Preparation of nanocellulose-polyvinyl alcohol composite hydrogels from Desmodium intortum (Mill.) Urb.: Chemical property characterization. *Industrial Crops and Products*, 176, 114371. <https://doi.org/10.1016/j.indcrop.2021.114371>
- Giusti, M. M., & Wrolstad, R. E. (2001). Characterization and measurement of anthocyanins by UV-visible spectroscopy. *Current protocols in food analytical chemistry*, 1, F1-2.
- Haro, D., Marquina-Barrios, S., Fuentes-Olivera, A., Quezada, A., Cruz-Monzón, J., Cueva-Almendras, L., Morán-González, C., entura-Avalos, Y. V., Rojas-Fermin, J., & Barraza-Jáuregui, G. (2024). Compositional and structural characterization of eleven types of lignocellulosic biomass and its potential application in obtaining nanopolysaccharides and producing polyhydroxyalkanoates. *Scientia Agropecuaria*, 15(4), 513-523. <https://doi.org/10.17268/sci.agropecu.2024.038>
- He, Y., Lu, L., Lin, Y., Li, R., Yuan, Y., Lu, X., Zou, Y., Zhou, W., Wang, Z., & Li, J. (2022). Intelligent pH-sensing film based on polyvinyl alcohol/cellulose nanocrystal with purple cabbage anthocyanins for visually monitoring shrimp freshness. *International Journal of Biological Macromolecules*, 218, 900-908. <https://doi.org/10.1016/j.ijbiomac.2022.07.194>
- Jiang, W., & Gu, J. (2020). Nanocrystalline cellulose isolated from different renewable sources to fabricate natural rubber composites with outstanding mechanical properties. *Cellulose*, 27(10), 5801-5813. <https://doi.org/10.1007/s10570-020-03209-3>
- Khalil, H. P. S. A., Yahya, E. B., Tajarudin, H. A., Surya, I., Muhammad, S., & Fazita, M. R. N. (2023). Enhancing the properties of industrial waste nanocellulose bioaerogels using turmeric nano particles. *Industrial Crops and Products*, 197, 116500. <https://doi.org/10.1016/j.indcrop.2023.116500>
- Koshy, R. R., K. V., Reghunadhan, A., Mary, S. K., Koshy, J. T., D. S., Williams, P. G., & Pothan, L. A. (2024). Biofilms from poly-vinyl alcohol/palmyra root sprout with Boswellia serrata, carbon dots and anthocyanin for sensing the freshness of sardine fish. *International Journal of Biological Macromolecules*, 273, 132991. <https://doi.org/10.1016/j.ijbiomac.2024.132991>
- Lee, H., You, J., Jin, H.-J., & Kwak, H. W. (2020). Chemical and physical reinforcement behavior of dialdehyde nanocellulose in PVA composite film: A comparison of nanofiber and nanocrystal. *Carbohydrate Polymers*, 232, 115771. <https://doi.org/10.1016/j.carbpol.2019.115771>
- Li, L., Wang, W., Sun, J., Chen, Z., Ma, Q., Ke, H., & Yang, J. (2022). Improved properties of polyvinyl alcohol films blended with aligned nanocellulose particles induced by a magnetic field. *Food Packaging and Shelf Life*, 34, 100985. <https://doi.org/10.1016/j.fpsl.2022.100985>
- Li, L., Wang, W., Zheng, M., Sun, J., Chen, Z., Wang, J., & Ma, Q. (2023). Nanocellulose-enhanced smart film for the accurate monitoring of shrimp freshness via anthocyanin-induced color changes. *Carbohydrate Polymers*, 301, 120352. <https://doi.org/10.1016/j.carbpol.2022.120352>
- Lim, H. J., Tang, S. Y., Chan, K. W., Manickam, S., Yu, L. J., & Tan, K. W. (2024). A starch/gelatin-based Halochromic film with black currant anthocyanin and Nanocellulose-stabilized cinnamon essential oil Pickering emulsion: Towards real-time Salmon freshness assessment. *International Journal of Biological Macromolecules*, 274, 133329. <https://doi.org/10.1016/j.ijbiomac.2024.133329>
- Liu, H., Shi, C., Sun, X., Zhang, J., & Ji, Z. (2021). Intelligent colorimetric indicator film based on bacterial cellulose and pelargonidin dye to indicate the freshness of tilapia fillets. *Food Packaging and Shelf Life*, 29, 100712.
- Mahardika, M., Masruchin, N., Amelia, D., Ilyas, R. A., Septevani, A. A., Syafri, E., Hastuti, N., Karina, M., Khan, M. A., Jeon, B.-H., & Sari, N. H. (2024). Nanocellulose reinforced polyvinyl alcohol-based bio-nanocomposite films: Improved mechanical, UV-light barrier, and thermal properties. *RSC Advances*, 14(32), 23232-23239. <https://doi.org/10.1039/D4RA04205K>
- Nagarajan, K. J., Balaji, A. N., & Ramanujam, N. R. (2019). Extraction of cellulose nanofibers from cocos nucifera var aurantiaca peduncle by ball milling combined with chemical treatment. *Carbohydrate polymers*, 212, 312-322.
- Nasution, H., Yahya, E. B., Abdul Khalil, H. P. S., Shaah, M. A., Suriani, A. B., Mohamed, A., Alfatah, T., & Abdullah, C. K. (2022). Extraction and isolation of cellulose nanofibers from carpet wastes using supercritical carbon dioxide approach. *Polymers*, 14(2), 326.
- Oktya, C., Kahyaoglu, L. N., & Moradi, M. (2023). Food freshness monitoring using poly(vinyl alcohol) and anthocyanins doped zeolitic imidazolate framework-8 multilayer films with bacterial nanocellulose beneath as support. *Carbohydrate Polymers*, 319, 121184. <https://doi.org/10.1016/j.carbpol.2023.121184>
- Panda, P. K., Sadeghi, K., & Seo, J. (2022). Recent advances in poly (vinyl alcohol)/natural polymer based films for food packaging applications: A review. *Food Packaging and Shelf Life*, 33, 100904. <https://doi.org/10.1016/j.fpsl.2022.100904>
- Patil, S., Bharimalla, A. K., Nadanathangam, V., Dhakane-Lad, J., Mahapatra, A., Jagajanantha, P., & Saxena, S. (2022). Nanocellulose reinforced corn starch-based biocomposite films: Composite optimization, characterization and storage studies. *Food Packaging and Shelf Life*, 33, 100860. <https://doi.org/10.1016/j.fpsl.2022.100860>
- Qiao, J., Dong, Y., Chen, C., & Xie, J. (2024). Development and characterization of starch/PVA antimicrobial active films with controlled release property by utilizing electrostatic interactions between nanocellulose and lauroyl arginate ethyl ester. *International Journal of Biological Macromolecules*, 261, 129415. <https://doi.org/10.1016/j.ijbiomac.2024.129415>
- Sarwar, M. S., Niazi, M. B. K., Jahan, Z., Ahmad, T., & Hussain, A. (2018). Preparation and characterization of PVA/nanocellulose/Ag nanocomposite films for antimicrobial food packaging. *Carbohydrate polymers*, 184, 453-464.
- Yan, J., Cui, R., Tang, Z., Wang, Y., Wang, H., Qin, Y., Yuan, M., & Yuan, M. (2021). Development of pH-sensitive films based on gelatin/chitosan/nanocellulose and anthocyanins from hawthorn (*Crataegus scabrifolia*) fruit. *Journal of Food*

- Measurement and Characterization*, 15(5), 3901-3911. <https://doi.org/10.1007/s11694-021-00978-8>
- Yu, K., Yang, L., Zhang, S., Zhang, N., Xie, M., & Yu, M. (2024). Stretchable, antifatigue, and intelligent nanocellulose hydrogel colorimetric film for real-time visual detection of beef freshness. *International Journal of Biological Macromolecules*, 268, 131602. <https://doi.org/10.1016/j.ijbiomac.2024.131602>
- Zevallos, L., Caldas, C., Flores, A., Obregón, J., Miano, A. C., & Barraza-Jáuregui, G. (2020). Mixing Design for Optimizing Ultrasound-Assisted Extraction of Phenolic Components and Anthocyanins from Blue Berries and Grape Marc. *International Journal of Fruit Science*, 20(sup3), S1313-S1327. <https://doi.org/10.1080/15538362.2020.1785987>
- Zhai, X., Shi, J., Zou, X., Wang, S., Jiang, C., Zhang, J., Huang, X., Zhang, W., & Holmes, M. (2017). Novel colorimetric films based on starch/polyvinyl alcohol incorporated with roselle anthocyanins for fish freshness monitoring. *Food Hydrocolloids*, 69, 308-317. <https://doi.org/10.1016/j.foodhyd.2017.02.014>
- Zheng, R., Liao, G., Kang, J., Xiong, S., & Liu, Y. (2024). An intelligent myofibrillar protein film for monitoring fish freshness by recognizing differences in anthocyanin (*Lycium ruthenicum*)-induced color change. *Food Research International*, 192, 114777. <https://doi.org/10.1016/j.foodres.2024.114777>
- Zhu, L., Feng, L., Luo, H., Dong, R., Wang, M., Yao, G., & Chen, J. (2022). Characterization of polyvinyl alcohol-nanocellulose composite film and its release effect on tetracycline hydrochloride. *Industrial Crops and Products*, 188, 115723. <https://doi.org/10.1016/j.indcrop.2022.115723>